

ELASTIC SCATTERING OF ANTI-PROTONS ON POLARIZED
PROTONS AT 1.73, 2.13, 2.37 AND 2.97 GeV/c

C. Daum, F.C. Erné^{*)}, J.P. Lagnaux^{**)},
J.C. Sens^{*)}, M. Steuer^{***)} and F. Udo^{*)}

CERN, Geneva, Switzerland

ABSTRACT

Differential cross-section and polarization distributions are presented for elastic $\bar{p}p$ scattering at incident momenta of 1.73, 2.13, 2.37 and 2.97 GeV/c. The data have been analysed in terms of a 5-parameter diffraction model. In terms of this model the difference in the shape of the differential cross-sections for $\bar{p}p$ and pp elastic scattering is a result of the strong absorption in the $\bar{p}p$ system.

(Submitted to Nuclear Physics)

Geneva - June 1968

-
- ^{*)} Visitor from the Foundation for Fundamental Research of Matter (F.O.M.), The Netherlands.
- ^{**)} Visitor from the Institut Interuniversitaire des Sciences Nucléaires, Bruxelles.
- ^{***)} Visitor from the Institute for High-Energy Physics of the Austrian Academy of Sciences, Vienna.

Faint header text at the top of the page, possibly containing a title or reference number.

Second line of faint text, likely a subtitle or introductory sentence.

Third line of faint text, continuing the introductory or header information.

Fourth line of faint text, possibly the start of a paragraph or section.

Fifth line of faint text, continuing the main body of the document.

Sixth line of faint text, providing further details or context.

Seventh line of faint text, likely a continuation of the previous section.

Eighth line of faint text, possibly a transition or a new point.

Ninth line of faint text, continuing the narrative or argument.

Tenth line of faint text, providing more information or examples.

Eleventh line of faint text, likely a summary or conclusion of a point.

Twelfth line of faint text, possibly a final sentence or a closing remark.

Thirteenth line of faint text, likely a signature or a reference.

Fourteenth line of faint text, possibly a date or a location.

Fifteenth line of faint text, likely a footer or a page number.

Sixteenth line of faint text, possibly a note or a reference.

Seventeenth line of faint text, likely a closing or a signature.

Eighteenth line of faint text, possibly a final note or a page number.

ELASTIC SCATTERING OF ANTIPROTONS ON POLARIZED
PROTONS AT 1.73, 2.13, 2.37 AND 2.97 GeV/c

C. Daum, F.C. Erné^{*)}, J.P. Lagnaux^{**)}
J.C. Sens^{*)}, M. Steuer^{***)} and F. Udo^{*)}
CERN, Geneva, Switzerland

1. EXPERIMENT

In this paper we report measurements of the angular distributions of the polarization and the differential cross-section in the elastic scattering of antiprotons on polarized protons at incident momenta of 1.73, 2.13, 2.37 and 2.97 GeV/c. Preliminary results have been reported elsewhere¹⁾.

The data have been taken in the course of an experiment on the elastic scattering of negative kaons on polarized protons²⁾. Since priority was given to the kaon experiment, the statistics obtained on the \bar{p} polarizations are somewhat marginal; the results are presented here, since no angular distributions of polarizations have been reported prior to this experiment³⁾. In the region of 1 to ~ 4 GeV/c, differential cross-sections have been reported at 1.5, 1.6, 1.7, 2.0, 2.5, 2.7, 3.0, 3.6, 3.66, and 4 GeV/c⁴⁾.

The experiment has been performed in a separated beam at the CERN Proton Synchrotron by recording coincidences between elastically-scattered antiprotons and recoil protons in counter hodoscopes placed around an LMN-type polarized target⁵⁾ in which the direction of the spin of the free protons was reversed once every few hours at each momentum. The target polarization was typically 65%.

The apparatus as well as the procedure followed in the analysis was identical in the K^- and p experiments and is described in Ref. 2. The

*) Visitor from the Foundation for Fundamental Research of Matter (F.O.M.), The Netherlands.

***) Visitor from the Institut Interuniversitaire des Sciences Nucléaires, Bruxelles.

****) Visitor from the Institute for High-Energy Physics of the Austrian Academy of Sciences, Vienna.

rate of antiprotons focused on the target was 3,000-10,000 per burst; data were collected for ~ 15 hours per momentum. A difference with the K^- experiment is the absence of regions, in the $\bar{p}p$ case, where elastic scattering is kinematically indistinguishable from "reverse-elastic" scattering in which the emerging antiproton and proton are interchanged. The angular distribution is thus measured twice, once with antiprotons going to the left, and once with them going to the right of the beam axis. This permits a check on an eventual vertical polarization of the incident \bar{p} beam; no such polarization has been observed. Another feature characteristic of the \bar{p} experiment is the strong absorption of the scattered antiprotons by the polarized target; the required correction to the rate of events is angle-dependent and reaches a maximum of 8%. All other corrections were the same as those applied to the K^- data.

The results are presented in Tables 1 and 2 and Figs. 1 and 2. In the figures the data points with spacing less than 0.035 in $\cos \vartheta_{c.m.}$ have been replaced by their weighted averages. The conversion to mb/sr has been obtained by extrapolating the forward region of the angular distribution to a point at 0° and using the optical theorem with total cross-section data taken from Abrams et al.⁶⁾. For this extrapolation the (nearly constant) slopes of the forward peaks in the data of Ref. 4 have been averaged and used for fitting through the few available forward points in our data. The uncertainty in this procedure results in an uncertainty in the vertical scale of $\pm 15\%$. This error is not included in the errors in the tables. The errors in the total cross-sections of Ref. 6 could be neglected.

The data show at all momenta a predominantly positive polarization, i.e. of the same sign^{*)} as the proton-proton polarization in this region of momenta. The polarizations reach maximum values of 15 to 35% in the diffraction region, then decrease towards a first minimum, but do not become strongly negative as, for example in the K^-p data. In the backward region ($\cos \vartheta_{c.m.} < -0.4$) the trend is lost due to poor statistics.

*) For the $\bar{p}p$ data the "Basel Convention" has been followed: the polarization is positive if, for target spin up, the incident particle is preferentially scattered to the left, looking along the downstream direction of the incident beam.

The angular distributions show the well-known diffraction peak, followed by a rather weak dip, a secondary maximum and possibly more dips. The first dip coincides rather well with the first minimum in the polarization curves. The first dip is at $-t = 0.5 - 0.6 \text{ (GeV/c)}^2$, independent of incident momentum. The differential cross-sections of Ref. 4 show a similar behaviour.

2. INTERPRETATION

The shape of the differential cross-sections of this experiment, as well as those of Ref. 4, suggests that a diffraction model can be applied to interpret the results. The incident momenta of this experiment seem rather low for a straightforward application of Regge pole predictions. In fact, by extrapolating calculations by Rarita et al.⁷⁾ to the present range of momenta one obtains polarizations with sign opposite to those of the data. On the other hand the resonance structure suggested by recent total cross-section data⁶⁾ is too weak to be observable with the accuracy of the present data.

Diffraction models including spin-flip amplitudes have been developed by Greider and Glassgold⁸⁾, McIntyre et al.⁹⁾ and by Frahn and Venter¹⁰⁾. These models are useful if the number of partial waves participating in the interaction is not too small. These conditions are satisfied in the case of low-energy scattering of nucleons and composite particles on nuclei (for which the models were first developed) and in the case of high-energy scattering of strongly interacting particles on nucleons. A specific circumstance in the latter case is the absence of Coulomb effects except in the very forward region.

Antiproton-proton scattering in the 1-3 GeV/c region seems suitable for this type of analysis since up to $l = 5$ waves participate in the interaction. We have therefore examined in some detail the model proposed by Frahn and Venter, which is sufficiently general to include several other models as special cases. The model has been published in detail for the (spin-0, spin-0) and the (spin-0, spin- $1/2$) cases; in adapting it to the (spin- $1/2$, spin- $1/2$) case several new parameters enter into the problem. Since the data do not allow anything more than a qualitative comparison with theory, we have restricted the number of parameters by the simplifying assumption that spin-spin interactions can be neglected compared to spin-orbit interactions. With this restriction, and the requirement of invariance

under rotation, reflection, time reversal and charge conjugation the scattering matrix is given by

$$M = f(\vartheta) + g(\vartheta) (\vec{\sigma}_1 + \vec{\sigma}_2) \cdot \hat{n} . \quad (1)$$

Here $f(\vartheta)$ and $g(\vartheta)$ are the non-flip and spin-flip amplitudes respectively; \hat{n} is a unit vector in the direction $\vec{k}_i \times \vec{k}_f$ (k_i, k_f are the initial and final momenta of the antiproton, respectively).

The differential cross-section and the polarization are given by:

$$\frac{d\sigma}{d\Omega} = |f|^2 + 2|g|^2 \quad (2)$$

$$P = 2 \operatorname{Re}(fg^*) / (|f|^2 + 2|g|^2) . \quad (3)$$

The functions $f(\vartheta)$ and $g(\vartheta)$ can be expanded in terms of four non-zero (3 triplet and one singlet) partial wave amplitudes¹¹⁾ for each ℓ , of which only two are independent:

$$f(\vartheta) = \frac{1}{k} \sum_{\ell} \left[(\ell + 1) R_{\ell, \ell+1}^T + \ell R_{\ell, \ell-1}^T \right] P_{\ell}(\cos \vartheta) \quad (4)$$

$$g(\vartheta) = \frac{i}{2k} \sum_{\ell} \left[R_{\ell, \ell+1}^T - R_{\ell, \ell-1}^T \right] P_{\ell}^1(\cos \vartheta) . \quad (5)$$

Here $R_{\ell, \ell \pm 1}^T$ are the triplet partial wave amplitudes for orbital angular momentum ℓ in the parallel (+) and antiparallel (-) configurations. They are related to the phase-shift parameters $\eta_{\ell, J}$ by:

$$R_{\ell, \ell \pm 1}^T = (\eta_{\ell, \ell \pm 1}^T - 1) / 2i . \quad (6)$$

In a simplified version of the Frahn-Venter model we have parametrized the partial wave amplitudes as follows:

$$\operatorname{Re} \eta_{\ell, \ell \pm 1} = \operatorname{Re} \eta_{\ell} = h(t) + \epsilon[1 - h(t)] \quad (7)$$

$$\operatorname{Im} \eta_{\ell, \ell \pm 1} = \mu^{\pm} \frac{dh}{dt} \quad (8)$$

where h is a continuous function of $t = l + 1/2$ and approximates a unit step function at $kR = l_{\max} + 1/2$; k is the wave number of the incident particle in the c.m. system and R the radius of interaction. The results are not very sensitive to the functional form of $h(t)$; a suitable form is given by:

$$h(t) = [1 + \exp (kR - t)/kd]^{-1}. \quad (9)$$

The parameters μ^{\pm} are a measure of the contributions to the real parts of the scattering amplitudes from the two spin states. The parameter ϵ provides for the transparency of the nucleon for lower l -waves. A diffuseness parameter d describes the transition from maximum to zero absorption. The behaviour of $\text{Re } \eta_l$ and $\text{Im } \eta_l$ versus l is analogous to the dependence of the "central" and "spin-orbit coupling" parts of the potential in the original model of Fermi¹²). In particular the form of Eq. (8) ensures that the polarization is a result of spin-dependent diffraction scattering from the surface of the region of interaction. Equations (2) and (3) have been fitted to the data using a standard fitting programme in which the parameters R , d , ϵ , μ^{\pm} were varied.

The results are presented in the upper part of Table 3 and Figs. 1 and 2. In Table 3 are indicated the best fitted values of the parameters R , d , μ^+ , μ^- and ϵ .

From the entries in Table 3 one notes first of all the stability of the parameters R and d , i.e. of the shape of the curve $\text{Re } \eta$ versus l as a function of momentum [see Eqs. (7) and (8)]. Apparently the imaginary part of the scattering amplitude remains substantially constant when the momentum increases. The experimental polarization is mainly positive giving rise to the result that μ^+ is larger than μ^- in all fits. In terms of potentials this means that the effective potential is stronger in the "parallel" than in the "antiparallel" state, and thus that the spin-orbit part of the potential is negative. The solution for μ^+ and μ^- presented in the table is not unique; $d\sigma/d\Omega$ is not sensitive to the sign of μ^+ and μ^- , and P is only sensitive to the sign of the difference of μ^+ and μ^- . Another solution exists, in which μ^+ and μ^- are negative, but still $\mu^+ > \mu^-$. The parameter ϵ is small compared to one indicating that the absorption is strong.

It is of interest to check if the same model can account also for pp scattering, though with different parameters. Figure 3 shows the results obtained in fitting pp data at 1.7, 2.1 and 3.0 GeV/c incident momenta. The data are taken from Ref. 13. The parameters obtained are listed in the lower part of Table 3. One notes a much smaller interaction radius, a larger value of d and a larger value for the opacity parameter ϵ , indicating a smaller, less-well defined interaction region with a weaker absorption. The difference of μ^+ and μ^- has the same sign as in $\bar{p}p$ scattering. The near absence of dips in the pp differential cross-section appears to be correctly described.

The model discussed here is a simplified version of the parametrization of Frahn and Venter. In the complete version the parameters ϵ , R and μ are all made distinct for the two spin states. In the present simplification the polarization is given in terms of $\mu^+ - \mu^-$ only. This choice is based on the general shape of the polarization distribution where no large positive to negative oscillations are observed¹⁰⁾. A consequence of the restrictions imposed is that the model cannot simultaneously account for the small-angle and large-angle regions of the distributions. The parameters of Table 3 describe the large-angle part ($-t \gtrsim 0.3 \text{ GeV}^2/c^2$) of the distributions only; to accommodate the small-angle features (slope of the forward peak, total cross-section, ratio of real to imaginary part of the scattering amplitude) as well, more parameters are required. The data points in the present experiment have large spacings and do not go beyond $\cos \theta \approx 0.9$; it thus seems appropriate to defer an over-all fit to the available information in this energy range until further, forthcoming measurements, both on $d\sigma/d\Omega$ and P , have been done.

In summary one might conclude that a relatively simple diffraction model, which allows for a real part in the scattering amplitude and allows for absorption which gradually varies with impact parameter, can reasonably well account for $\bar{p}p$ elastic scattering and pp elastic scattering in the region of a few GeV/c incident momenta. There is in fact a notable similarity between the differential elastic cross-sections and polarizations in $\bar{p}p$ scattering at the momenta of this experiment and the scattering of, for example, 180 MeV protons on light nuclei¹⁴⁾. On the other hand, the Regge pole model, as formulated in Ref. 7 and when extrapolated down to the range of momenta of the present experiment, is in disagreement with the sign of $\bar{p}p$ polarizations observed.

Acknowledgements

We wish to thank Mr. M. Arbet for his able assistance in the course of this experiment. We are very much indebted to Messrs. M. Borghini, J. Conciencia, O. Runolfsson, M. Uldry, and J. Vermeulen for setting up and maintaining the polarized target; their untiring and competent assistance has been a vital element in the performance of the experiment. We thank Messrs. S. Andersson and G. Plaut for their contributions to the analysis of the data. We are pleased to acknowledge the support given to the experiment by Professors W. Paul, P. Preiswerk and A.H. Wapstra. This work was supported in part by the Stichting voor Fundamenteel Onderzoek der Materie (F.O.M.), which is supported by the Nederlandse Organisatie voor Zuiver Wetenschappelijk Onderzoek (Z.W.O.).

REFERENCES

- 1) L. di Lella, Proceedings of the Heidelberg International Conference on elementary particles (1967), p. 159.
- 2) C. Daum, F.C. Ern , J.P. Lagnaux, J.C. Sens, M. Steuer and F. Udo, to be published in Nuclear Physics.
- 3) Polarizations, averaged over the forward peak region, have been published by J. Button and B. Magli , Phys.Rev. 127, 1297 (1966), L. Dobrzynski, C. Ghesquiere, Ng.H. Kuong and H. Tafte, Physics Letters 23, 614 (1966), and B. Escoubes et al., Physics Letters 5, 132 (1963).
- 4) B. Barish, D. Fong, R. Gomez, D. Hartill, J. Pine and A.V. Tollestrup, Phys.Rev. Letters 17, 720 (1966) [1.5, 2.0 and 2.5 GeV/c]; G.R. Lynch, R.E. Foulks, G.R. Kalbfleish, S. Limentani, J.B. Shafer, M.L. Stevenson and Ng.H. Kuong, Phys.Rev. 131, 1276 (1963) [1.61 GeV/c]; V. Domingo, G.P. Fisher, L. Marshall Libby and R. Sears, Physics Letters 24B, 642 (1967) [2.7 GeV/c]; B. Escoubes et al., Physics Letters 5, 132 (1963) [3.0 GeV/c and 3.6 GeV/c]. W.M. Katz et al., UR-875-201 [3.66 GeV/c]. R. Armenteros, C.A. Coombes, B. Cork, G.L. Lambertson and W.A. Wenzel, Phys.Rev. 119, 2068 (1960). O. Czyzowski et al., Physics Letters 15, 188 (1965) [4 GeV/c].
- 5) M. Borghini, P. Roubeau and C. Ryter, Nucl.Instr.Meth. 49, 248 (1967); Nucl.Instr.Meth. 49, 259 (1967).
- 6) R.J. Abrams, R.L. Cool, G. Giacomelli, T.F. Kycia, B.A. Leontic, K.K. Li and D.N. Michael, Phys.Rev. Letters 18, 1209 (1967).
- 7) W. Rarita, R.J. Riddell, C.B. Chiu and R.J.N. Phillips, University of California Radiation Laboratory Report, UCRL 17523 (unpublished).
- 8) K.R. Greider and A.E. Glassgold, Ann.Phys. (N.Y.) 10, 100 (1960).
- 9) J.A. McIntyre, K.H. Wang and L.C. Becker, Phys.Rev. 117, 1337 (1960).
- 10) W.E. Frahn and R.H. Venter, Ann.Phys. (N.Y.) 27, 135 (1964); Ann.Phys. (N.Y.) 27, 385 (1964); Ann.Phys. (N.Y.) 27, 401 (1964).
- 11) M.H. MacGregor, M.J. Moravcsik and H.P. Stapp, Ann.Rev.Nucl.Sci. 10, 291 (1960).
- 12) E. Fermi, Nuovo Cimento, 11, 407 (1954).
- 13) M.J. Longo, M.A. Neal and O.E. Overseth, Phys.Rev. Letters 16, 536 (1966); J.D. Dowell, W.R. Frisken, G. Martelli, B. Musgrave, H.B. van der Raay and R. Rubinstein, Nuovo Cimento 18, 818 (1960); S.P. Kushinin et al., Sov.J. Nuclear Physics 1, 225 (1965); B. Cork, W.A. Wenzel and C.W. Causey, Phys.Rev. 107, 859 (1957); M.J. Longo and B.J. Moyer, Phys.Rev. 125, 701 (1962).
- 14) A. Johansson, U. Svanberg and P.E. Hodgson, Arkiv Fysik 19, 541 (1961); A. Johansson, U. Svanberg and O. Sundberg, Arkiv Fysik 19, 527 (1961).

Table captions

Tables 1 and 2 : Differential cross-sections and polarizations with errors at 1.73, 2.13, 2.37 and 2.97 GeV/c incident \bar{p} momenta. The cross-sections (column SIGMA) and the errors in the cross-sections (column DSIGMA) are given in mb/sr. The uncertainty in scale of $\pm 15\%$ on the cross-sections is not included in the errors.

Table 3 : Diffraction scattering parameters obtained for $\bar{p}p$ and pp elastic scattering. The parameters are defined in the formulas (6) to (9) in the text. The pp data are taken from Ref. 13.

Table 1

INCIDENT MOMENTUM =1730.0 MEV/C
CENTER OF MASS MOMENTUM= 695.0 MEV/C

COS	POL	DPOL	SIGMA	DSIGMA
0.899	0.27	0.08	57.453	27.536
0.889	0.12	0.06	28.214	7.285
0.847	0.33	0.04	11.196	0.809
0.824	0.28	0.04	7.715	0.553
0.746	0.34	0.07	2.313	0.188
0.596	0.66	0.62	0.144	0.071
0.563	0.55	0.17	0.310	0.045
0.501	0.29	0.17	0.446	0.064
0.409	0.45	0.15	0.360	0.048
0.393	0.11	0.14	0.472	0.061
0.271	0.26	0.12	0.572	0.062
0.244	0.19	0.16	0.328	0.046
0.141	0.62	0.17	0.337	0.050
0.069	0.33	0.21	0.226	0.041
0.000	0.45	0.19	0.234	0.037
-0.099	0.52	0.23	0.172	0.032
-0.153	0.18	0.21	0.189	0.035
-0.267	0.57	0.50	0.054	0.022
-0.301	-0.25	0.40	0.064	0.022
-0.422	-0.32	0.65	0.060	0.035
-0.452	-0.33	0.41	0.074	0.027
-0.570	1.16	1.13	0.048	0.035
-0.596	-0.82	0.61	0.060	0.029
-0.727	0.49	0.71	0.056	0.033

INCIDENT MOMENTUM =2130.0 MEV/C
CENTER OF MASS MOMENTUM= 807.0 MEV/C

COS	POL	DPOL	SIGMA	DSIGMA
0.902	0.12	0.04	17.056	3.452
0.896	0.18	0.04	17.442	2.616
0.829	0.18	0.03	7.782	0.578
0.706	0.24	0.10	0.841	0.093
0.635	0.29	0.16	0.557	0.081
0.555	0.11	0.11	0.497	0.056
0.546	0.02	0.12	0.602	0.073
0.441	0.14	0.12	0.557	0.064
0.393	0.23	0.11	0.496	0.054
0.321	-0.01	0.13	0.376	0.046
0.223	0.27	0.13	0.299	0.037
0.196	0.25	0.20	0.208	0.037
0.055	0.29	0.17	0.185	0.028
0.050	-0.10	0.21	0.163	0.031
-0.094	0.07	0.28	0.110	0.028
-0.121	-0.02	0.32	0.091	0.026
-0.249	0.03	0.35	0.075	0.024
-0.281	-0.07	0.32	0.095	0.027
-0.407	0.06	0.28	0.093	0.023
-0.430	0.19	0.48	0.066	0.028
-0.562	-0.16	0.29	0.105	0.027
-0.568	0.69	0.55	0.084	0.037
-0.694	-0.39	0.75	0.057	0.038
-0.699	-0.82	0.81	0.041	0.026

Table 2

INCIDENT MOMENTUM =2370.0 MEV/C
CENTER OF MASS MOMENTUM= 870.0 MEV/C

COS	POL	DPOL	SIGMA	DSIGMA
0.903	0.22	0.04	20.165	4.398
0.889	0.19	0.04	13.929	1.978
0.791	0.22	0.09	1.966	0.242
0.702	0.19	0.13	0.740	0.102
0.660	-0.21	0.14	0.687	0.100
0.549	0.01	0.11	0.752	0.093
0.380	0.29	0.11	0.661	0.082
0.352	0.35	0.18	0.460	0.077
0.227	0.44	0.26	0.242	0.055
0.207	-0.15	0.15	0.395	0.058
0.088	0.09	0.30	0.171	0.045
0.034	-0.29	0.36	0.118	0.036
-0.062	-0.26	0.51	0.079	0.035
-0.135	0.09	0.32	0.130	0.036
-0.218	-0.07	0.26	0.151	0.035
-0.296	0.09	0.31	0.145	0.040
-0.580	14.88	218.88	0.003	0.049
-0.704	19.88	156.98	0.007	0.068

INCIDENT MOMENTUM =2970.0 MEV/C
CENTER OF MASS MOMENTUM=1011.0 MEV/C

COS	POL	DPOL	SIGMA	DSIGMA
0.923	0.09	0.03	24.571	5.225
0.828	0.17	0.05	6.336	0.570
0.741	0.13	0.16	0.820	0.136
0.691	-0.09	0.11	0.992	0.116
0.618	0.03	0.15	0.893	0.121
0.526	-0.05	0.10	0.955	0.109
0.525	0.17	0.15	0.857	0.120
0.417	0.13	0.21	0.343	0.063
0.344	0.14	0.17	0.376	0.058
0.294	0.05	0.22	0.357	0.068
0.165	-0.52	0.38	0.171	0.054
0.161	-0.12	0.23	0.293	0.059
0.012	-0.42	0.38	0.150	0.048
-0.011	-0.09	0.27	0.190	0.044
-0.146	0.44	0.66	0.074	0.042
-0.319	-2.23	2.66	0.037	0.041
-0.336	-0.08	1.04	0.057	0.054
-0.480	-0.71	1.23	0.043	0.041
-0.483	0.92	0.62	0.068	0.031
-0.606	0.40	1.31	0.073	0.084
-0.640	0.29	1.06	0.046	0.043
-0.783	1.21	3.24	0.026	0.053
-0.893	0.76	2.93	0.040	0.091

Table 3

Parameters of modified Frahm-Venter model
for best fit to $\bar{p}p$ and pp elastic scattering data

Data	R (fm)	d (fm)	μ^+	μ^-	ϵ
$\bar{p}p$ 1.73 GeV/c a)	1.08	0.13	0.86	0.00	0.07
$\bar{p}p$ 2.13 GeV/c a)	1.03	0.11	0.82	0.41	0.04
$\bar{p}p$ 2.37 GeV/c a)	1.03	0.11	0.93	0.34	0.00
$\bar{p}p$ 2.97 GeV/c a)	0.97	0.09	0.98	0.73	0.00
pp 1.70 GeV/c b)	0.62	0.19	3.42	-0.95	0.37
pp 1.73 GeV/c c)					
pp 2.20 GeV/c b)	0.64	0.15	3.57	-1.24	0.54
pp 2.08 GeV/c c)					
pp 3.04 GeV/c b)	0.73	0.18	5.01	-1.57	0.72
pp 2.99 GeV/c c)					

a) Differential cross-section + polarization distribution

b) Differential cross-section

c) Polarization distribution

Figure captions

- Fig. 1 : Differential elastic cross-sections and polarizations at 1.73 and 2.13 GeV/c. The mb/sr scale is uncertain by $\pm 15\%$. The lines indicate the fit with the parameters of Table 3.
- Fig. 2 : Differential elastic cross-sections and polarizations at 2.37 and 2.97 GeV/c. The mb/sr scale is uncertain by $\pm 15\%$. The lines indicate the fit with the parameters of Table 3.
- Fig. 3 : Proton-proton differential cross-section and polarization data from Ref. 13. The lines indicate the best fit with the same model as used for the $\bar{p}p$ data of this experiment, with parameters given in Table 3.

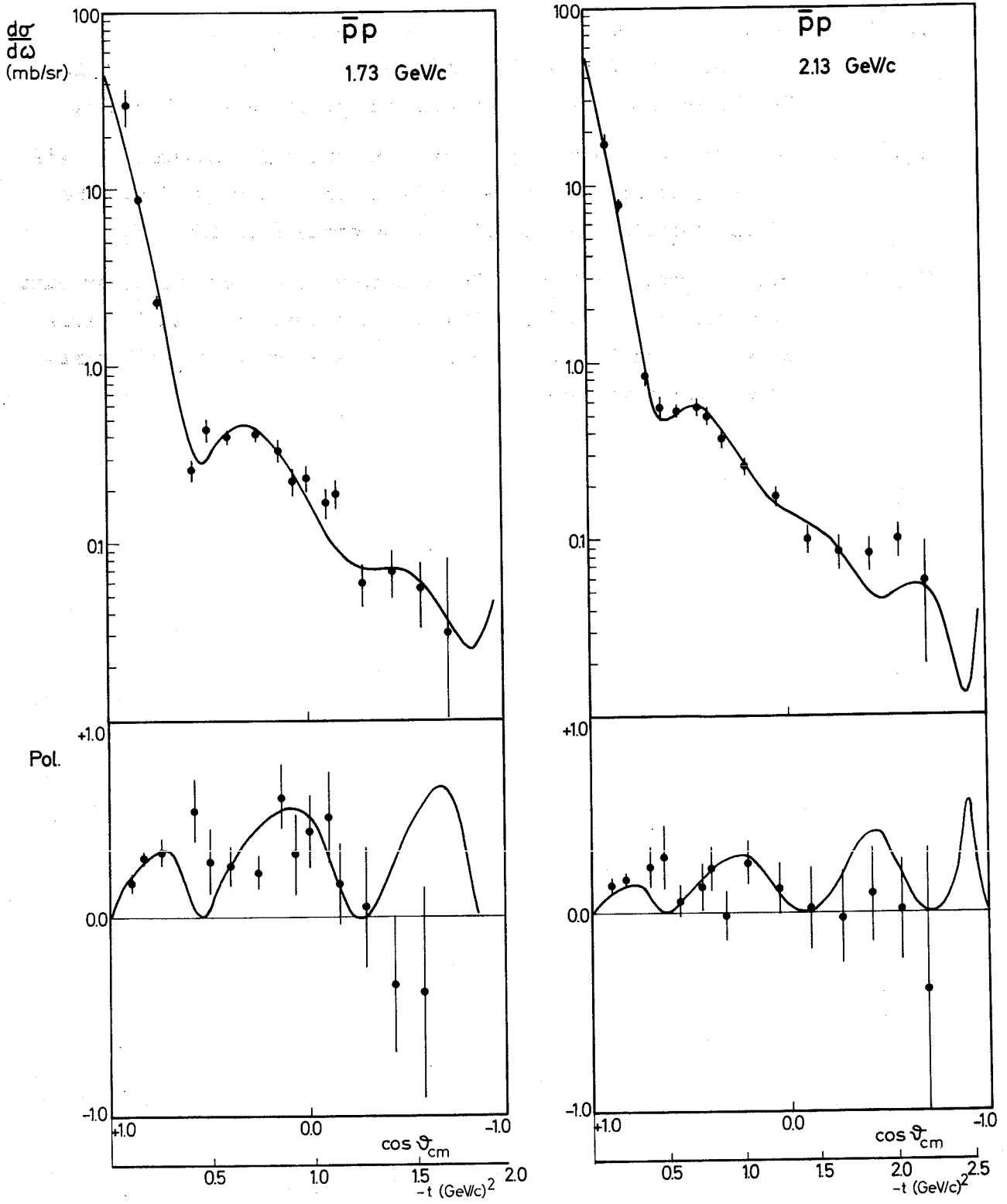


Fig. 1

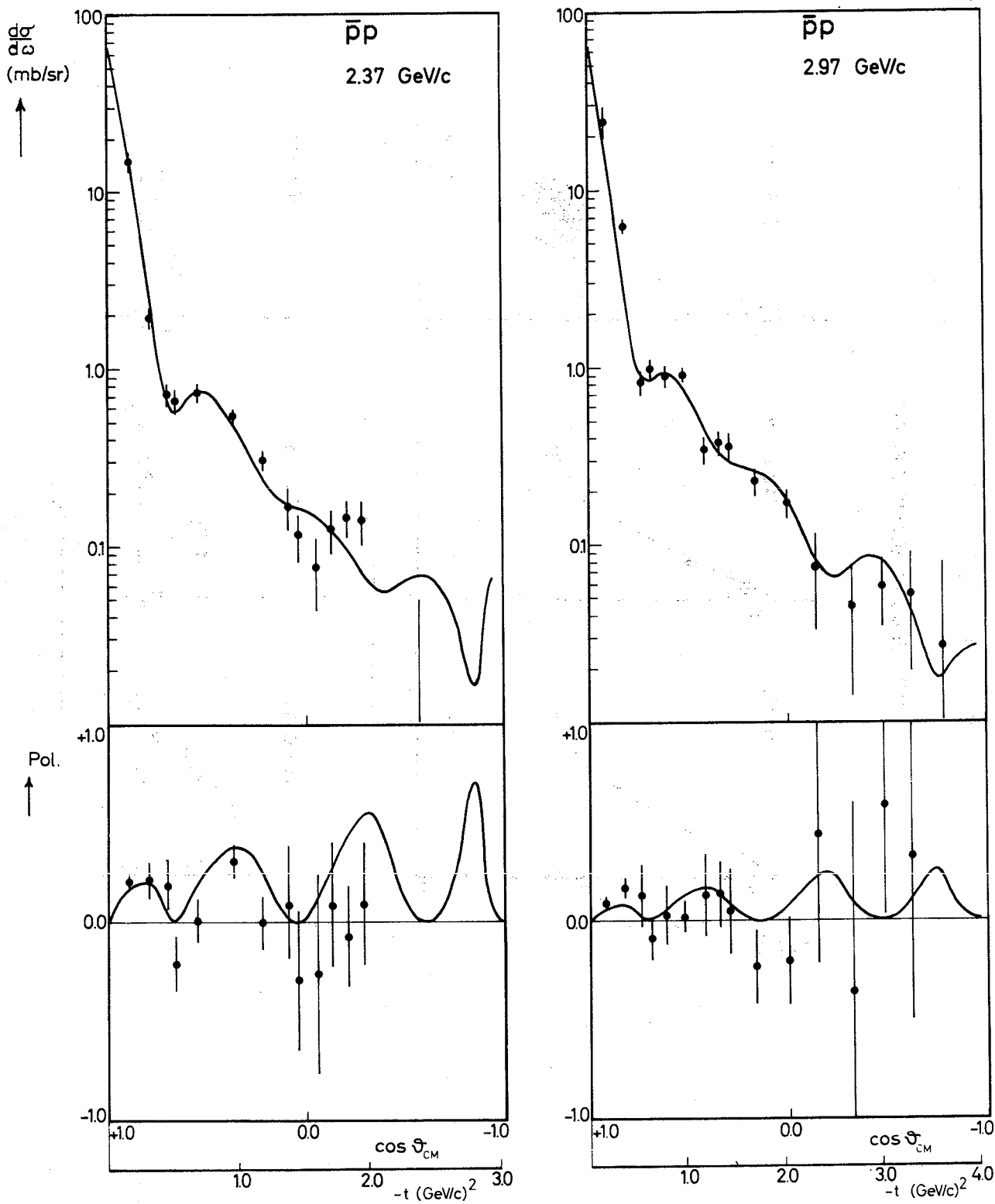


Fig. 2

PP ELASTIC SCATTERING FITS

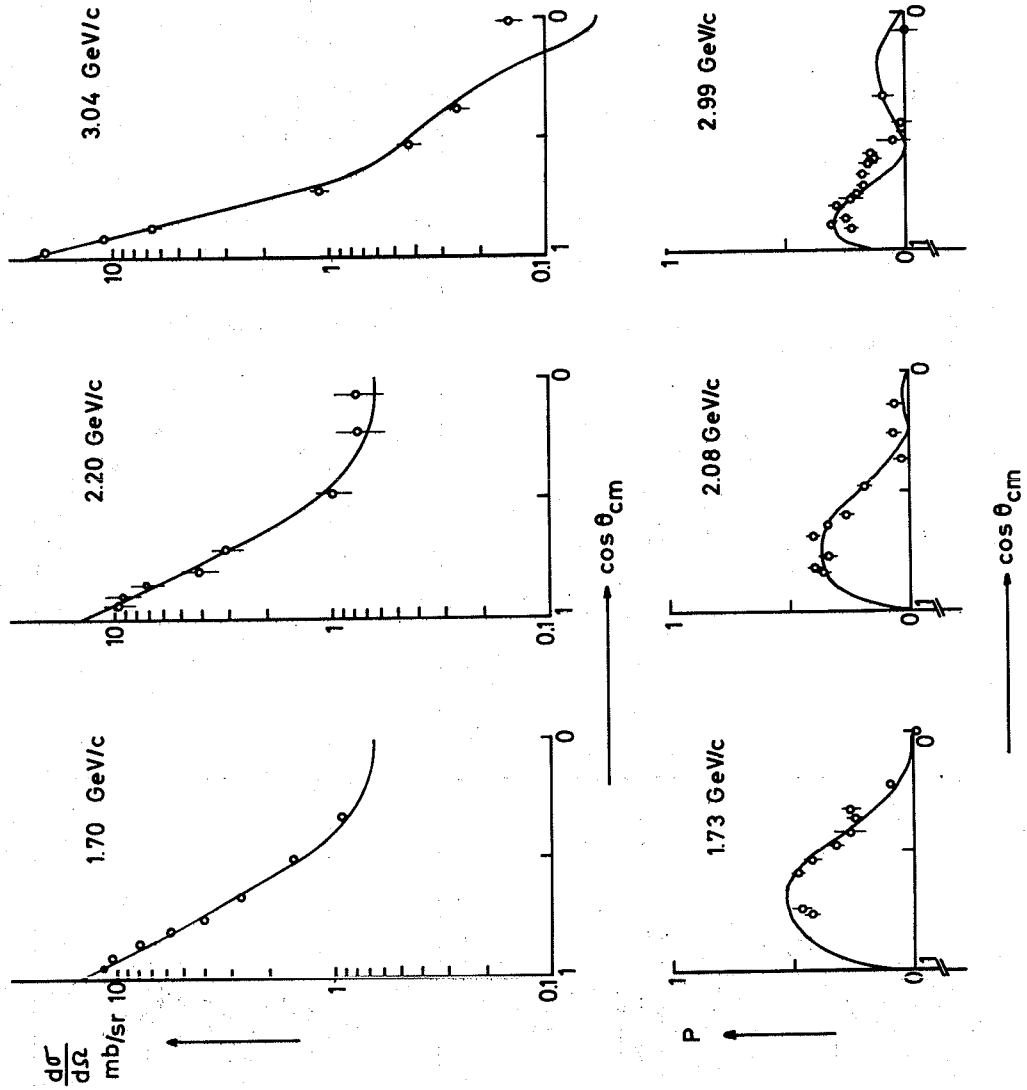


Fig. 3



1911

C

C

1911